Nature of Protons, Phase Transitions, and Dynamic Disorder in Poly- and Oligoaniline Bases and Salts: An Inelastic Neutron Scattering Study

A. El Khalki† and Ph. Colomban*

Nanophases and Heteregeneous Solids Group, LADIR UMR 7075 CNRS & University Pierre et Marie Curie, 2 rue Henry-Dunant, 94320 Thiais, France

B. Hennion

Léon Brillouin Laboratory, CEA-CNRS, CEA-Saclay, Bat 563, 91191 Gif-sur-Yvette Cedex, France

Received October 23, 2001; Revised Manuscript Received April 2, 2002

ABSTRACT: An inelastic neutron scattering study of polyaniline (camphorsulfonic and chloride salts, emeraldine base in the form of powder or film) from ca. 1 to 120 cm^{-1} shows significant changes in the compounds as a function of the temperature. Intensity and bandwidth undergo major modifications below 50 K, because of the freezing of the dynamic ring disorder. The greatest modifications were observed for camphorsulfonic acid salt. In the range from 100 to 3000 cm^{-1}, a nonlocalized inelastic scattering process previously assigned to the "free protons" (in other words, noncovalently bonded hydrogen atoms) was also observed. Comparison with the spectra of oxidized tetramer (BQBBa), BB (diphenylamine), BBB (*N*,*N*′-diphenyl-1,4-phenylenediamine), and BQB (-diimine) model compounds shows that, at the neutron spectrometer resolution, the dynamics of BQB already give a good basis for the aromatic ring dynamics in a polyaniline framework. Assignment of the modes is proposed in the light of low-wavenumber Raman and IR spectra. The thermal disordering of the rotational degrees of freedom appears very similar to that observed in crystalline benzene.

Introduction

Over the past few decades, conducting polymers, including polyaniline, have been the objects of intensive research. The conductivity of polyaniline depends on the degree of oxidation and of protonation of the polymeric backbone. It varies by 10 orders of magnitude when the semioxidized form, the so-called emeraldine base (EB), is fully protonated to form emeraldine salt (ES, in which the cation is the "protonated" polymeric chain). This transformation can also be described as acid intercalation between the polymeric chains. The fully oxidized form is pernigraniline, and the fully reduced form is called leucoemeraldine. The studies of polyanilines have for a long time been hampered by the absence of clear information on their short- and medium-range structure. The crystallinity of polyaniline is as best as 50%,[1,2] and the low stability of the materials under an electron beam has prevented any accurate investigation. However, in a recent high-resolution electron microscopy study,[3] on samples selected on the basis of Raman spectroscopy results for their 'high" crystalline state, we showed that the materials consist in rolled "sheets" (20−100 nm in diameter), with an amorphous surface layer of varying thickness. Almost periodic growth irregularities are currently observed. This spherical or tubular habit is consistent with the great similarity of polyaniline X-ray powder patterns to those of fibrous aluminosilicates: all patterns show tailed reflections spread out in directions corresponding to increasing values of 2Θ, which arise from the numerous stacking faults and from the curvature.

Vibrational spectroscopy is well established as a good method for the study of the short-range order and structure of poorly crystallized, or even amorphous, materials. In a previous work we used Raman spectroscopy to investigate in the low- and intermediate-wavenumber regions,[4] and we obtained indirect information about the chain organization. However, the huge Rayleigh scattering hinders the analysis below ∼100 cm^{-1}, even using high-resolution spectrometers equipped with holographic gratings and liquid nitrogen-cooled, back-illuminated, CCD detectors. This huge Rayleigh scattering was assigned to the strong optical heterogeneity arising from the coexistence of conducting and insulating regions within the materials. Furthermore, the structure difference between the amorphous skin of spherules/tubes and their crystalline core explains the large discrepancy in Raman spectra recorded with different exciting laser lines. This is because the penetration depth of the excitation light varies as a function of the exciting wavelength (electronic absorption). Because the interaction between matter and neutrons is only a function of the atom nucleus, the heterogeneous "electrooptic" character of polyaniline does not affect inelastic neutron scattering. The scattering cross section of hydrogen atoms is about 10 times greater than that of C and N atoms; protonic motions will therefore dominate the spectra. Proton dynamics in polyanilines have been studied above 100 cm^{-1} so far. Satisfactory test measurements[4] merit further investigation.

The numerous publications on polyaniline's properties include reports on the large changes in thermoelectric power,[5,6] spin behavior,[7,8] and electrical conductivity[9,10] between ca. 100 and 10 K. Analysis of the low-wavenumber vibrational spectrum as a function of temperature will offer a chance of understanding the resulting

† On leave from Laboratoire de Physique du Solide, Faculté des Sciences Dahr el Mehraz, Fez, Maroc.

* Corresponding author: e-mail colomban@glvt-cnrs.fr; fax 33 1 4978 1118.

10.1021/ma011837x CCC: $22.00
Published on Web 05/24/2002

structural changes and detect any phase transition, ordering, etc. We chose to use a three-axis spectrometer at the Léon-Brillouin Laboratory for the following reasons. First, the location of the spectrometer is very close to the neutron reactor, which offers a flux competitive with that available on spectrometers illuminated by a spallation source (Isis-Rutherford Appleton Laboratory, UK) or a high-flux reactor (Laüe-Langevin, F). Three-axis spectrometers are mainly devoted to measurements on single crystals. This is the best instrument allowing a point-by-point investigation of (Q,ω) space, and consequently, this class of instrument is a very powerful tool for the study of phase transitions (pretransitional behaviors and microscopic mechanisms). Another advantage of this type of spectrometer is the possibility of collection of both phonon and Bragg peaks, in successive runs on the same sample.

In this paper we compare the temperature evolution of inelastic (and elastic) neutron scattering (INS) spectra of the oxidized tetramer BQBBa [a stands for a terminal amine group, the polyaniline schematic unit being BQBB (B for benzenic rings, Q for a quinoid ring, the nitrogen atom in between is not represented)] and the corresponding BB (diphenylamine), BBB (*N,N′*-diphenyl-1,4-phenylenediamine), and BQB (*N,N′*-diphenyl-1,4-phenylenediimine) model compounds with those of emeraldine base and salts (chloride and camphorsulfonic acids). The fully oxidized polymer, pernigraniline ((BQ)n), and solid benzene (B) are also used for comparison. Samples are in the form of powders or ground films; a mosaic stack of emeraldine chloride films is also considered. Assignments are discussed in light of IR and Raman measurements in the low-wavenumber region.

Experimental Section

Samples. The synthesis of pristine emeraldine chloride (ES-I form) and of base powder (EB-I form) has been described extensively in a previous paper.[4] The emeraldine base film was prepared from an EB-I solution in *N*-methyl-2-pyrrolidinone by slow evaporation in air.[1,4] Protonation was achieved in chloride acid, following the previous descriptions.[1−4] The preparation of camphorsulfonic acid derivative was made by mixing the emeraldine base with camphorsulfonic acid in *m*-cresol and subsequent slow evaporation in air, following ref 11. The film was hand-ground in an agate mortar (platelets < 1 mm^2). Two kinds of fibers, one prepared from a gel of CSA, *m*-cresol, and emeraldine chloride at room temperature (fiber 1) and the other from a gel made using emeraldine base and heated to ca. 100 °C (fiber 2), were spun in acetone. Diphenylamine (BB) was used as received from Fluka Chemie, CH (#42750, purity 99%). Details about the recrystallization of the *N,N′*-diphenyl-1,4-phenylenediamine (BBB) and -diimine (BQB) have already been given.[4] The tetramer BQBBa was prepared as described by Zhang et al.[12] The Service Central d'Analyse du CNRS (69 Vernaison, France) checked chemical composition for many batches.

Techniques. Inelastic and elastic (i.e., diffraction) neutron scattering measurements were carried out on the 4F2 triple-axis spectrometer, installed on the cold source of the Orphée reactor at the Laboratoire Léon Brillouin, Saclay (France). The neutron beam was delivered by a double monochromator, using the pyrolytic graphite (002) reflection (PG002). The use of a triple-axis spectrometer allowed us to collect data at constant momentum transfer $|Q|$. We used a constant final wave vector $k_f = 1.64$ A^{-1}, with a PG002 analyzer bent horizontally for focusing, which yielded an energy resolution of ~0.05 THz (0.2 meV, 1.6 cm^{-1}) at the elastic position. A graphite filter placed behind the sample prevented high-order contamination; 1.5−3 g of sample was contained in an aluminum cylinder closed with a screwed aluminum stopper.

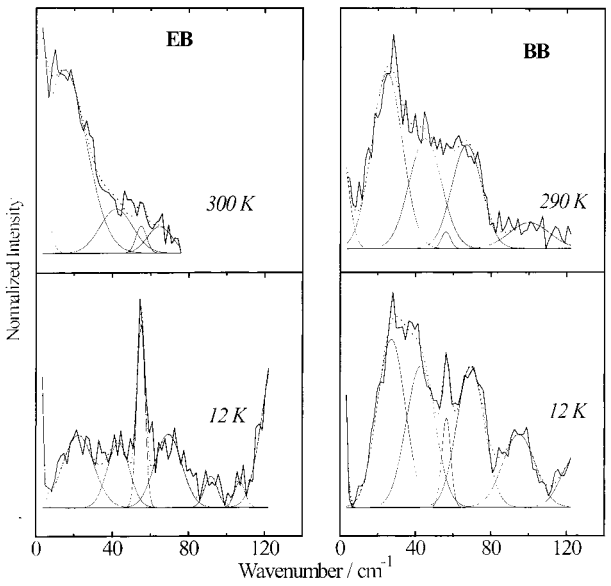

Figure 1. Inelastic neutron scattering spectra of emeraldine base (EB-I) and of diphenylamine (BB) at different temperatures. The 55 cm^{-1} narrow peak arises from the elastic neutron scattering from the aluminum container.

Closed-cycle, helium cryostats were used. Full stabilization within 1 K was required before each recording. Spectra were renormalized with respect to the weight of the sample placed in the beam.

An Infinity multichannel Dilor-Jobin-Yvon (Lille, France) Notch filtered spectrograph equipped with a Peltier cooled CCD matrix and an "*XY*" spectrograph (Dilor) equipped with a double monochromator filter and a back-illuminated, liquid nitrogen-cooled, 2000 × 800 pixels CCD detector (Spex, the Jobin-Yvon Co., France) were used to record Raman spectra. A microconfiguration, using an Olympus microscope (long focus Leitz objective, magnification ×500, confocal setting) and 457.1 or 647 nm exciting lines (0.01−0.1 mW) allowed recording down to ca. 30 cm^{-1}.

IR reflection spectra were recorded down to 50 cm^{-1} using a Fourier transform Bruker 113V interferometer. The spectra were converted to the absorption scale using the Bruker OPUS software.

Fitting Procedure. Fitting of the various spectral components using Origin software (MicroCal Inc., USA) started with the selection of a restricted working window, followed by the choice of the bands to be fitted. The bands were characterized by their widths at half-maximum and their forms assumed to be pure Gaussian (for INS except for the elastic line considered as a Lorentzian) or pure Lorentzian (for Raman spectra).

Results and Discussion

Temperature Evolution. Figures 1, 2, and 3 show the inelastic neutron scattering spectra of emeraldine base, chloride, and CSA salts at different temperatures between 1.5 (or 12) and 300 K. Similar features, more or less pronounced, are observed for all compounds: (i) a gap appears below 50 K between the softest band at about 20 cm^{-1} and the elastic peak; (ii) simultaneously, the scattered intensity increases above 80 cm^{-1} (Figure 4). Note that the narrow peak at ca. 55 cm^{-1} clearly observed in the low-temperature spectra and the strong one at ca. 120 cm^{-1} are due to the residual elastic contribution of the aluminum container. Examination of the (elastic) diffraction patterns recorded after each inelastic spectrum run (Figure 5) shows that no major structural change takes place for BB, BBB, and BQB compounds. On the other hand, a marked narrowing of BQBBa and EB patterns is observed when the temper-

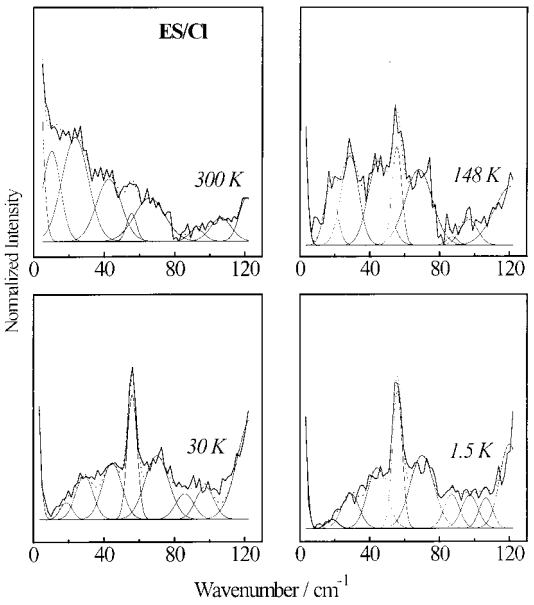

Figure 2. INS spectra of emeraldine chloride powder (ES-I) at various temperatures.

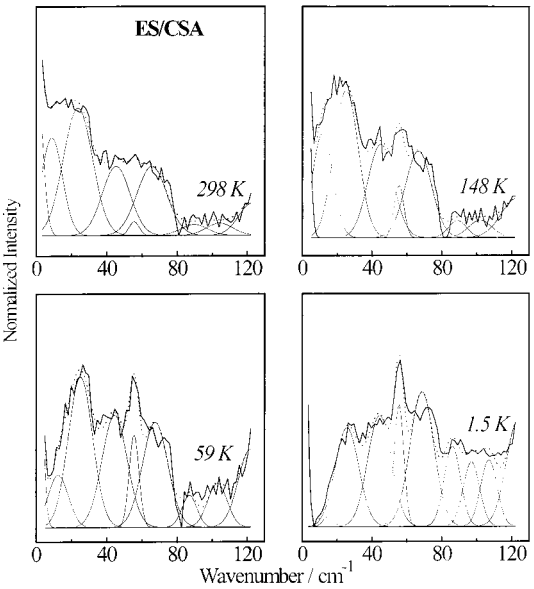

Figure 3. INS spectra of emeraldine camphorsulfonic acid ground film (ES/CSA) at different temperatures.

ature is reduced. A very similar feature is observed when we consider samples of variable crystallinity.[13] The broad bumps in the 300 K EB spectrum are resolved at 12 K into a structured massif rather similar to that of BQBBa. Such narrowing could indicate a decrease in dynamical disorder. The diffraction peaks of these compounds remain broad, characteristic of poorly crystallized material. Interreticular distances correspond well to those reported from previous X-ray investigations.[13−16]

A rather similar sequence is visible if we compare the set of inelastic spectra recorded at RT for BBB, BQB, BQBBa, and (BQ)n (see below). The gap between the elastic peak and the first mode reduces when the number of aromatic rings increases or when the temperature is increased. The ca. 25−30 cm^{-1} band wavenumber softens, and its intensity increases. As previously observed, the crystallinity of pernigraniline ((BQ)n) is significantly better than that of emeraldine forms.

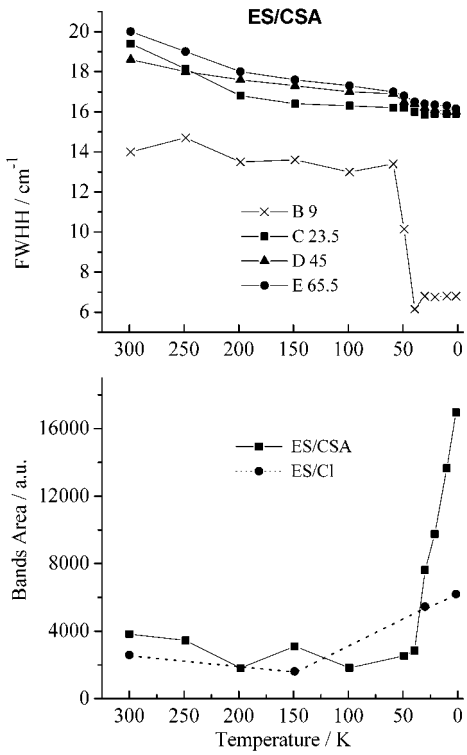

Figure 4. Plots of the full width at half-height (fwhh) of band at ca. 9 (B), 23.5 (C), 45 (D), and 65.5 cm^{-1}(E) and band area above 80 cm^{-1} for ES/CSA spectra in comparison with data of emeraldine chloride.

Scaling Motif, Crystallinity, and Dynamic Disorder. Various kinds of heterogeneity and disorder are expected in the studied materials. The glass transition temperature (T_g) of long-chained polyaniline is close to 420 K,[3,17] but much lower values are expected for short-chain polymers and, furthermore, for the tetramer. A huge dynamic disorder is thus expected at 300 K. Furthermore, two families of polymorphs, the EBI/ESI and EBII/ESII forms, have been recognized.[1,4,18,19] High-resolution electron microscopy has clearly revealed that amorphous and "crystalline" zones are not located randomly: crystalline regions are located in the center of rolled sheets or clews. In contrast, the matter at the periphery is amorphous.[3] The size of "crystalline" regions (20−100 nm) roughly corresponds to the coherence lengths deduced from X-ray band shape analysis.[1,3] This does not imply that "ordered" and amorphous regions form a mosaic in real space. The crystalline layers are curved. Coherence lengths are calculated assuming that the peak broadening arises from limited crystallite size and not on the basis of von Hoseman's and Guinier's paracrystal description.[20,21] These authors proposed the model of the continuous deformation of the periodic crystal structure by replacing the constant cell edges by statistically determined vectors varying in length and direction. The individual cells thereby become deformed, and so does their content. The same scaling motif can be repeated over a limited distance, whatever the origin used. The model of a continuously connected network, where bond angles and bond lengths change within a certain limit, is consistent with (i) a curvature of chain planes (evidenced from high-resolution electron microscopy[3] and expected from the previous discussion of Poujet et al.[22]) and (ii) a plastic state (because of the vicinity of the softening temperature). This description is also consistent with the distribution of two kinds of

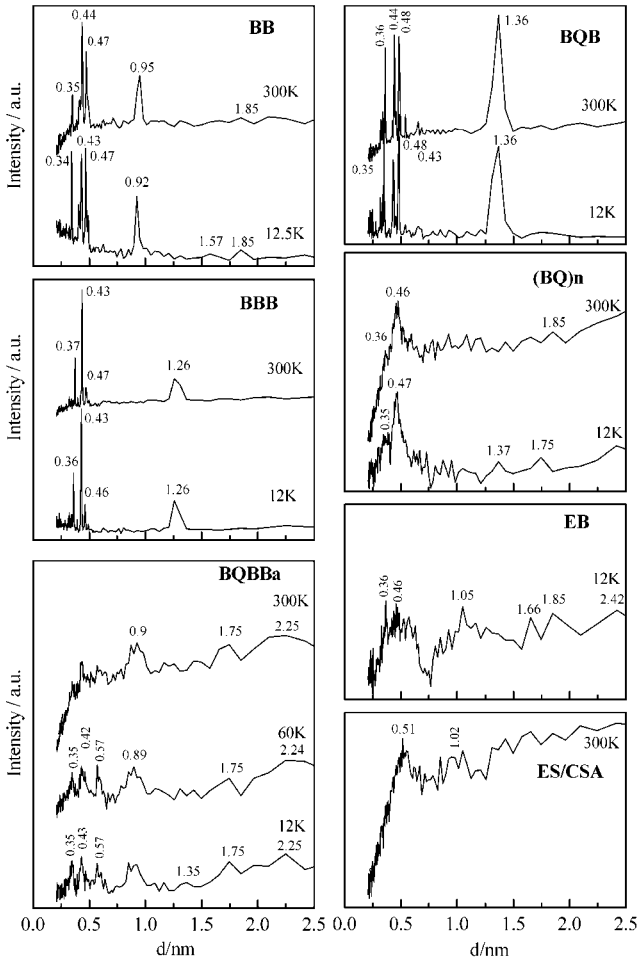

Figure 5. Neutron diffraction spectra recorded at different temperatures for BB, BBB, BQBBa, BQB, (BQ)n, EB-I, and ES/CSA samples (see text for the explanation of acronyms).

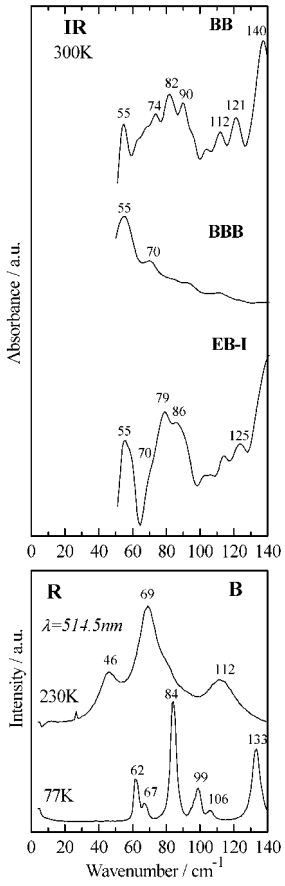

Figure 6. Room temperature IR absorption spectra for BB, BBB, and EB-I powders calculated from reflection measurements. Raman spectra of solid benzene are given for comparison.

rings (benzenoic "B" and quinoic "Q") along the chain which could provoke stress and hence curvature. The model of metallic islands in which charge hopping dominates, embedded in a poorly conducting zone, has been extensively used to describe the electrical properties,[23] but experimental identification of the crystalline regions as metallic islands failed. The size of such islands is expected to be of the order of 10^5-10^6 unit cells ($V_{\text{unit cell}} = \sim 0.5$ nm^3).[24,25] The size of crystalline regions ranges from 10^3 to 10^6 nm^3.[1,4] The model of chains entangled to form a "clew" has also been proposed without direct experimental evidence (but this description was useful to explain the "good" solvent effect of *m*-cresol).[26] Because of the strong electronic absorption, the temperature can be greatly increased under the laser spot, up to T_g. Previous Raman measurements show that the temperature of a laser-illuminated sample was close to 50 K even when the sample was immersed in liquid helium. A Raman study of the dynamics as a function of the temperature is thus not possible. A neutron investigation will help better to understand this material and to separate the dynamical from static disorder contributions.

Low Wavenumber Excitations: Comparison between IR, Raman, and INS Spectra of Polyanilines and Their Model Compounds. Although most vibrational studies deal with the stretching regions (>1000 cm^{-1}), a few papers report the low and medium wavenumber regions, using inelastic neutron,[27−29] IR,[4,18,30] and Raman scattering.[4,18] Stretching modes give information about the nature of the chemical bonds,[31,32] while bending modes (200−800 cm^{-1} region) are very useful for analyzing the short-range orientational order in relation with adjacent chains.[4] External and lattice modes, characteristic of the structural arrangement of the vibrational units, are expected below 200 cm^{-1}. A huge heterogeneity of the electromagnetic properties results from the different regions/islands composing the materials. This affects the IR absorption analysis of polyaniline salt dispersed, in KBr or ICs pellets, or paraffin oil: well-defined transmission windows arise from reflections at the interface between conducting and nonconducting regions,[19] perturbing the absorption curve of the conductive materials. For this reason, only the IR spectra of BB, BBB, and EB samples could be obtained from reflectance measurements (Figure 6, Table 1). This heterogeneity of the electromagnetic properties is also at the origin of the huge Rayleigh scattering wings extending up to 150 cm^{-1} [4] that prevents accurate measurements in the external and librational mode region. All IR spectra of conducting emeraldine salts exhibit a band at ca. 150 cm^{-1}. Its high intensity shows that all dipolar species (i.e., the anions and the cationic polymeric chain) are involved in this motion. Assignment to an interchain N−H···N bond has been proposed,[27] but it is rejected on the basis of inelastic neutron scattering analysis in the 200−3800 cm^{-1} range:[28,29] this mode involves coupled motion of chain vs anions. The observation of a medium-intensity INS counterpart indicates that hydrogen motion undergoes a small riding effect. However, when a hydrogen atom enters the electronic shell of a nitrogen (or oxygen)

Table 1. Low wavenumber IR, Raman and INS excitations measured at ~300 K and their assignments of polyanilines and their model compounds (see text for acronym explanation)

B		Aniline at 77K	BB			BBB			BQB		BQBBa	$(BQ)_n$	EB		BBB/Cl	ES-I/Cl			ES/CSA		BB solid		ES-I/Cl film	EB-II film	ES-I/Cl powder at 30K	Assignments
																					[35]		[4,18,30]	[4,18]	[27-29]	
IR	R	IR	IR	R	INS	IR	R	INS	R	INS	INS	INS	IR	INS	INS	IR	R	INS	R	INS	IR	R	IR	INS	INS	
							[9][a]				17	13		15	11			11		9						Translational motion of aromatics rings (T')
		29			25		22	26		27		27			24			24		24						
	46	45		41	45		38	41	45	43	41	44		42	44			43		45		40				
		51																								
		58	55	54	56[b]	55		55[b]	50	55[b]	55[b]	55[b]	55	55[b]	55[b]			55[b]		55[b]	54	55		56	d	
62		62																								Ring rotation (R')
67	69				67		62	66		68	67	67		64	66			66		66						
		70																								
		78	(74)[c]	79		(70)	75		73				79								73	79				
84		86	83				84		81				86											80		
99			(90)[c]					91	92	91	96	99			97		90	93	90		92	98			90	
		104		100			100	102																	102	Motion of [(BQB)-B] vs anion
106	112	108	112						112	110								106								
		120	121	129									123				120		125		111					
133		136	140																			131	140			
		147														150			148		139					

[a] Band observed at helium temperature. [b] Band assigned to residual elastic scattering of the aluminum container is present, especially at low temperature. [c] Shoulder can arise from interface. [d] Not studied below 90 cm^{-1}.

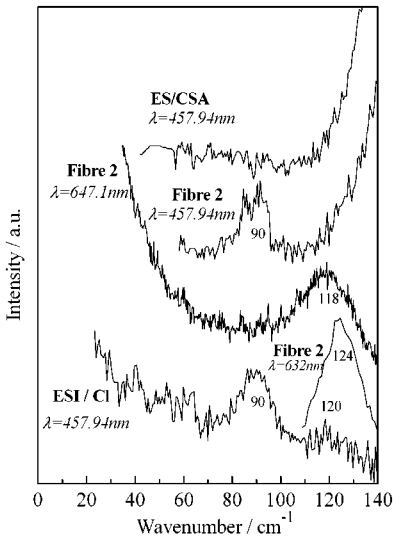

Figure 7. Comparison of the Raman spectra recorded on ES/CSA film and fibers with those of ES-I chloride film.

atom to form a covalent N−H (or O−H) entity, any motions of the heavy atom will impart the same displacement to the H atom, like a rider moving with his horse. On the contrary, the IR spectrum of the neutral emeraldine base[4] shows in the same range a very small peak with an additional band at ca. 80 cm^{-1}. All spectra show a narrow peak at ca. 55 cm^{-1} and additional components between 70 and 150 cm^{-1}, although artifacts cannot be excluded because we are very close to the limit of the instrument. As shown in Figure 7, the Raman spectra are complex. First, Raman intensity depends on the exciting wavelength and on the polarizability tensor of the chemical bond. If the laser photon energy approaches those of certain electronic states of material, then near-resonant/resonant Raman scattering occurs, and the scattered light intensity is increased. Usually, the Raman excitation energy ranges between 1 and 3 eV, i.e., in the range of optical absorption of either poly- or oligoanilines. The electronic band shape depends on the chain length, the degree of oxidization, and the protonation level.[33] The penetration depth can be limited to a few tens of nanometers in resonant materials, which makes Raman microscopy a surface analysis method. It is clear that Raman analysis requires the use of many exciting wavelengths to be significant and that the view will remain selective, especially in our case, because of the spherical/tubular habit, to the surface analysis. Thus, we will consider different spectra recorded on different types of materials (powders, films, fibers) in order to collect most of the Raman peaks. Furthermore, symmetry rules could involve IR/Raman exclusion for structures having a center of symmetry (e.g., for ES-I form[4,18]). Vibrational data and previous proposed assignments are summarized in Table 1.

Figures 7 and 8 show the comparison of Raman spectra of different polymer salts (CSA salt in the fibrous form, chloride salt in the form of powder or film) with those of BB, BBB, and BQB. A Raman spectrum of solid benzene (B) at 230 and 77 K is shown in Figure 6. The spectra of B and BQB are very similar (Figures 6 and 8). Wavenumber shift and band broadening were observed when temperature increased as the result of fast molecular reorientations of the benzene rings. For symmetry reasons only librational modes are active in solid benzene,[34] and thus the Raman triplet observed,

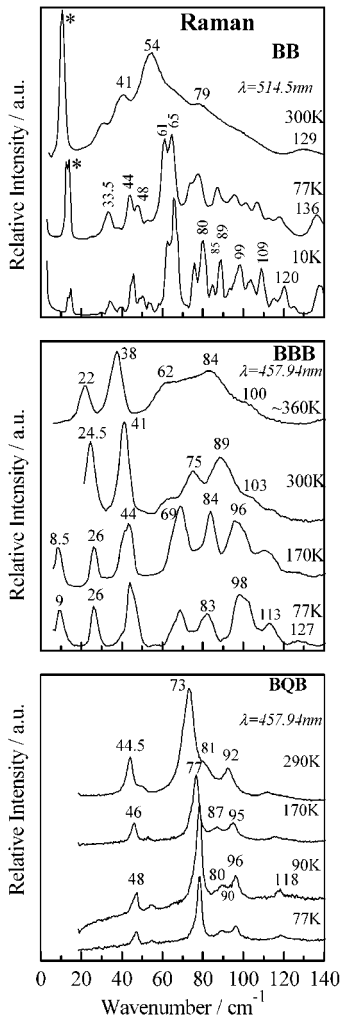

Figure 8. Comparison of the Raman spectra of BB, BBB, and BQB powders.

for all the model compounds but more or less resolved, can be assigned to ring librational mode. At 300 K, the broad triplet envelope is located at ca. 60 (BB), 70 (BBB, BQB), and 90 cm^{-1} (emeraldine salts). Similar peaks are observed in many derivatives.[35−38] Previous calculation[39] and discussion[4] support the assignment of these peaks to a Raman-active torsional mode in which adjacent rings oscillate out-of-phase. Such a motion originates from the coupled reorientation of the aromatic rings. If this assignment is correct, then the wavenumber increase [i.e., in the sequence BB/BQB/polyaniline, the triplet peak at ca. 54/73−84 (Figure 8)/90 (Figure 7)] indicates that the potential well of the rotation around C−N−C (C═N═C) bridges becomes stronger when the electronic delocalization extends over many rings.

Translational modes of benzene are only IR-active in solid benzene.[34] We would expect the Raman activity to remain low in model compounds and to have at least one translational modes located at a very low wavenumber. IR spectra show a feature at ca. 55 cm^{-1} (Figure 6), but modes at lower wavenumber are expected: modes close to 25 cm^{-1}, or less, are well observed in INS spectra (Figures 1−3 and 9, and 10). Assignment of thess peaks to translational modes of the chain portion is consistent because of their strong intensities. (The intensity of inelastic neutron peaks is strong for modes involving large displacement of the H

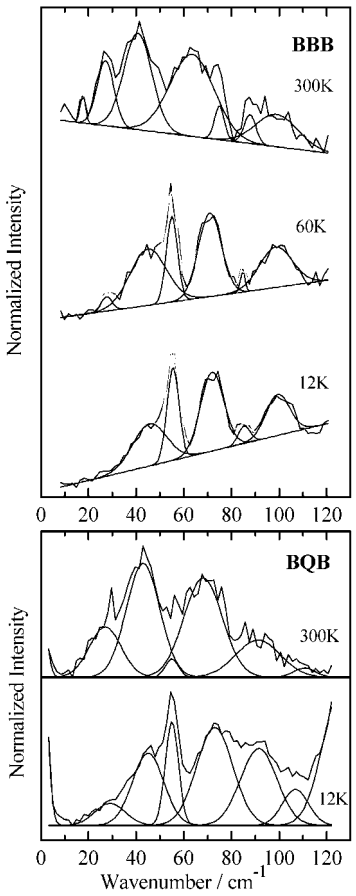

Figure 9. INS spectra of BBB and BQB powders at various temperatures.

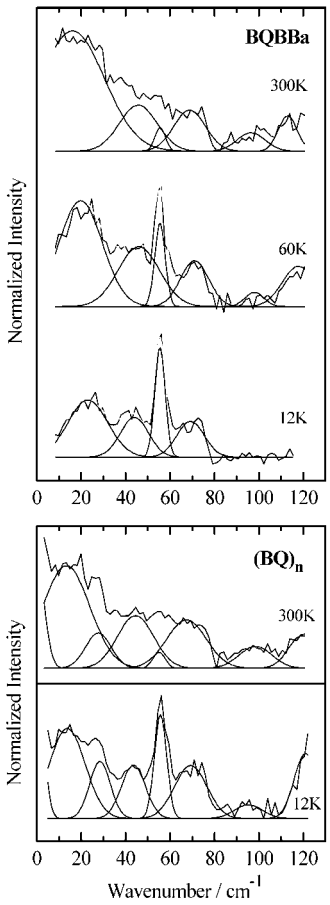

Figure 10. INS spectra of BQBBA and of pernigraniline ((BQ)n) powders.

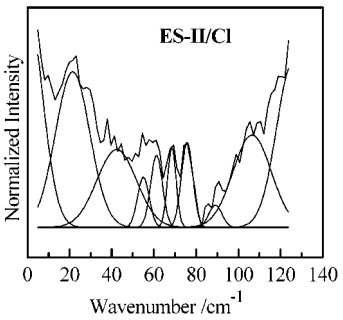

Figure 11. INS spectrum recorded at 300 K on a sample composed of a stack of the emeraldine chloride films.

atom and or motion of many H atoms, such as ring translations.)

Significant narrowing is observed on cooling for BB and BQB samples, but no band splitting is obvious. Thus, we can consider that the broadening of the 300 K spectra is due to dynamic disorder.

We now examine the spectra of BQB sample (Figure 9). Except for a new band at ca. 30 cm^{-1}, all INS peaks correspond to those seen in the Raman spectra (Figure 8), but their intensities are different. The strongest Raman peak (ca. 75−79 cm^{-1}) has a rather strong INS counterpart, according to a rotation of the aromatic rings. The strongest INS band peaks at ca. 40 cm^{-1}. The (BQ)n spectrum (Figure 10) looks very similar to that of the BQBBa tetramer, except that the band at 18−28 cm^{-1} softens and splits. A more structured spectrum is consistent with the higher crystallinity of pernigraniline. The lower wavenumber of this strong additional INS feature supports its assignment to a collective translation of the chain vibrational unit. A very low wavenumber band (ca. 10 cm^{-1}) is observed on the BBB Raman spectrum (Figure 8) and seems not to correspond to a plasma line. This range was not analyzed for the BQB sample for which peaks were visible only after opening the slit, which increases the Rayleigh wing. It is thus possible that a very low-energy excitation merges with the elastic peak in polymer Raman spectra because of the strong damping of this soft mode and the lower experimental resolution.

The spectrum recorded from an oriented sample (consisting of a stack of emeraldine chloride film pieces) exhibits rather well-defined peaks: a ∼20 cm^{-1} band is already well shaped at room temperature (Figure 11). This confirms the anisotropic and more ordered character of the films as observed by Sauvageol et al.[27] in the higher wavenumber range. Room-temperature wavenumber and assignments are summarized in Table 1.

Comparison between Highly Conducting Salts and the Poorly Conducting Polymer Base: The "Free" Proton Model. The second stringent phenomenon is the intensity above ca. 80 cm^{-1} at liquid helium temperature (see spectra in Figures 1−3 and intensity plot in Figure 4). In a previous examination at the Rutherford Appleton Laboratory (UK), with the TFXA spectrometer, a continuum above 100 cm^{-1} (assigned to "free" protons) was observed in the 20 K spectra.[28,29] The recording conditions hampered examination below ca. 100 cm^{-1}. New measurements can help to go further in the understanding of this phenomenon. Precluding any

interpretation, this energy range has been despicted in Figures 1−3 by a set of bands.

Two different types of protons are expected in our samples: (i) protons covalently bound to neighboring carbon and/or nitrogen atoms; (ii) protons not covalently bound to neighboring atoms, i.e., free from the dynamical point of view. Such protons are not observed with the IR technique and cannot be characterized unambiguously with diffraction or NMR techniques. Other possible detection techniques might include very accurate chemical/weight analysis.

We observe a rather flat feature of spectra above ca. 80 cm^{-1}. This suggests that some protons are trapped in a shallow potential, with a single state located at ca. 80 cm^{-1}, below the dissociation threshold. In this case, we can distinguish two dynamical regimes: the localized, covalently bound protons below 80 cm^{-1} and nearly free protons above that level.

Are these free protons the real charge carriers in proton conduction? How do free protons correlate with the electronic structure of the host? The existence of free protons in solids has been regarded for a long time as unlikely, but recent studies of disordered and mixed proton conductors[40,41] might bring the hypothesis back into favor.

The narrowing of the BQBBa, (BQ)n, and EB elastic neutron scattering peaks with decreasing temperature is consistent with a freezing of the dynamic disorder of the very short part of the chain. It is clear that the high dynamic disorder at room temperature limits the crystallinity, and the paracrystallinity model may prove in future studies. This is also consistent with the interest in synthesizing and conserving the materials at low temperature to preserve their crystallinity as well as the use of viscous solvent.

Conclusion

Major changes in the dynamics of hydrogen atoms as a function of temperature in oligo- and polyanilines have been evidenced. They are not only straightforward for highly conducting polyaniline (ES/CSA) but also for observation in model compound. The freezing of the dynamic disorder of B and Q rings was observed below 50 K. Also, an "anomalous" H scattering is observed above 80 cm^{-1}, in accordance with the previous investigations at 20 K by the TFXA spectrometer. This temperature range corresponds to the domain where polyaniline conductivity drops sharply. The dynamic rotational disorder of aromatic rings and the special character of some protons can be correlated with the electronic charge transport behavior. The spectrum of an oriented stack of emeraldine chloride films exhibits narrower features and an enhanced band at ca. 20 cm^{-1}. From the vibrational point of view, BQB and even to some extent solid benzene reflect most of the dynamics of the polymeric chain in the low-wavenumber region. This confirms our previous conclusion (based on the study of stretching and bending modes) that the vibrational unit consists of the BQB segment plus an isolated benzene ring (B).

Acknowledgment. Drs. S. Folch, N. Leygue, and Mr. F. Romain are gratefully acknowledged for their help in the sample synthesis and IR/Raman measurements. The authors thank Drs. A. Gruger and A. Regis for fruitful discussions.

References and Notes

(1) Pouget, J. P.; Jozefowicz, M. E.; Epstein, A. J.; Tang, X.; MacDiarmid, A. G. *Macromolecules* **1991**, *24*, 779−89.
(2) Maron, J.; Winokur, M. J.; Mattes, B. R. *Macromolecules* **1995**, *28*, 4475−86.
(3) Mazerolles, L.; Folch, S.; Colomban, Ph. *Macromolecules* **1999**, *32*, 8504−08.
(4) Colomban, Ph.; Folch, S.; Gruger, A. *Macromolecules* **1999**, *32*, 3080−92.
(5) Wang, Y. Z.; Joo, J.; Hsu, C.-H.; Epstein, A. J. *Synth. Met.* **1995**, *68*, 207−11.
(6) Kaiser, A. B.; Subramanian, C. K.; Gilberd, P. W.; Wessling, B. *Synth. Met.* **1995**, *69*, 197−200.
(7) Ginder, J. M.; Epstein, A. J. *Solid State Commun.* **1987**, *63*, 97−101.
(8) Sacricifti, N. S.; Kolbert, A. C.; Cao, Y.; Heeger, A. J.; Pines, A. *Synth. Met.* **1995**, *69*, 243−44.
(9) Kohlman, R. S.; Zibold, A.; Tanner, D. B.; Ihas, G. G.; Ishiguro, T.; Min, Y. G.; MacDiarmid, A. G.; Epstein, A. J. *Phys. Rev. Lett.* **1997**, *78*, 3915−18.
(10) Wessling, B.; Srinivasan, D.; Rangarajan, G.; Mietzner, T.; Lennartz, W. *Eur. Phys. J. E* **2000**, *2*, 207−10.
(11) Pouget, J. P.; Hsu, C.-H.; MacDiarmid, A. G.; Epstein, A. J. *Synth. Met.* **1995**, *69*, 119−20.
(12) Zhang, W. J.; Feng, J.; MacDiarmid, A. G.; Epstein, A. J. *Synth. Met.* **1997**, *84*, 119−20.
(13) Colomban, Ph.; Folch, S.; Gruger, A.; Regis, A. *C. R. Acad. Sci., Ser. IIb* **1996**, *322*, 63−70.
(14) Winokur, M. J.; Mattes, B. R. *Phys. Rev. B* **1996**, *54*, R12637−40.
(15) Laridjani, M.; Epstein, A. J. *Eur. Phys. J. B* **1999**, *7*, 585−97.
(16) Luzny, W.; Samuelsen, E. J.; Djurado, D.; Nicolau, Y. F. *Synth. Met.* **1997**, *90*, 19−23.
(17) Wei, Y.; Jang, G.-W.; Hsueh, K. F.; Scherr, E. M.; MacDiarmid, A. G.; Epstein, A. J. *Polym. Mater. Sci. Eng.* **1989**, *61*, 916−20.
(18) Folch, S.; Gruger, A.; Colomban, Ph. *J. Chim. Phys.* **1998**, *95*, 1299−1302.
(19) Colomban, Ph.; Gruger, A.; Regis, *C. R. Acad. Sci. Paris* **1995**, *T.321, Serie IIb*, 247−54.
(20) Von Hoseman, R. *Acta Crystallogr.* **1951**, *4*, 520−29.
(21) Von Hoseman, R.; Steffen, B. *The Phenomenon of Paracrystallinity in Review of the Hungarian Academy of Science, Budapest*, 1978.
(22) Pouget, J. P.; Oblakowski, Z.; Nogami, Y.; Albouy, P. A.; Lardjani, M.; Oh, E. J.; Min, Y.; MacDiarmid, A. G.; Tsukamoto, J.; Ishiguro, T.; Epstein, A. J. *Synth. Met.* **1994**, *65*, 131−40.
(23) Kohlman, R. S.; Epstein, A. J. In *Handbook of Conducting Polymers*; Marcel Decker: New York, 1997; Chapter 3, pp 85−121.
(24) Joo, J.; Oblakowski, Z.; Du, G.; Pouget, J. P.; Oh, E. J.; Wiesenger, M. Y.; MacDiarmid, A. G.; Epstein, A. J. *Phys. Rev. B: Rapid Commun.* **1994**, *49*, 2977−80.
(25) Wang, Z. H.; Scherr, E. M.; MacDiarmid, A. G.; Epstein, A. J. *Phys. Rev. B* **1992**, *45*, 4190−202.
(26) MacDiarmid, A. G.; Epstein, A. J. *Synth. Met.* **1994**, *65*, 103−16.
(27) Sauvageol, J. C.; Djurado, D.; Dianoux, A. J.; Fisher, J. E.; Scherr, E. M.; Macdiarmid, A. G. *Phys. Rev. B* **1993**, *47*, 4959−63.
(28) Baddour-Hadjean, R.; Fillaux, F.; Colomban, Ph.; Gruger, A.; Regis, A.; Parker, S. F.; Yu, L. T. *Synth. Met.* **1996**, *81*, 211−14.
(29) Fillaux, F.; Baddour-Hadjean, R.; Leygue, N.; Colomban, Ph.; Parker, S. F.; Gruger, A.; Regis, A.; Yu, L. T. *Chem. Phys.* **1997**, *216*, 281−93.
(30) Ghosh, S.; Bowmaker, G. A.; Cooney, R. P. *J. Mater. Chem.* **1997**, *7*, 597−600.
(31) Furakawa, Y.; Ueda, F.; Hyodo, Y.; Harada, I.; Nakajima, T.; Kawagoe, T. *Macromolecules* **1988**, *21*, 1297−305.
(32) Louarn, G.; Lapkowski, M.; Quillard, S.; Pron, A.; Buisson, J. P.; Lefranc, S. *J. Phys. Chem.* **1996**, *100*, 6998−7006.
(33) Folch, S.; Regis, A.; Gruger, A.; Colomban, Ph. *Synth. Met.* **2000**, *110*, 219−27.
(34) Sidorov, N. V.; Krasyukov, Yu. N.; Mukhatarov, E. I. *J. Appl. Spectrosc. (Russian Transl.)* **1999**, *66*, 423−30.

(35) Perrier-Datin, A.; Lebas, J. M. *J. Chem. Phys.* **1972**, *4*, 591−600.
(36) Tripathi, G. N. R. *J. Chem. Phys.* **1980**, *37*, 5521−30.
(37) Ohno, K.; Kimura, J.; Ymakita, Y. *Chem. Phys. Lett.* **2001**, *342*, 207−19.
(38) Maxton, P. M.; Schaeffer M. W.; Felker, P. M. *Chem. Phys. Lett.* **1995**, *241*, 603−10.
(39) Ginder, J. M.; Epstein, A. J. *Phys. Rev. B* **1990**, *B41*, 10674−85.
(40) Colomban, Ph.; Tomkinson, J. *Solid State Ionics* **1997**, *97*, 123−34.
(41) Colomban, Ph. *Ann. Chim. Sci. Mater.* **1999**, *24*, 1−18.

MA011837X